A glimpse into the future: The physics of hot and dense QCD matter

Alejandro Ayala

Instituto de Ciencias Nucleares, UNAM

ayala@nucleares.unam.mx

October 28, 2017

Guy Paic

Overview

1. QCD phase diagram
   - Finite temperature and vanishing baryon chemical potential
   - Non-vanishing baryon chemical potential: The sign problem.
2. QCD phase diagram from chiral symmetry restoration
   - Linear sigma model with quarks
   - Effective potential
3. Results: Critical End Point location
4. Conclusions

QCD phase diagram

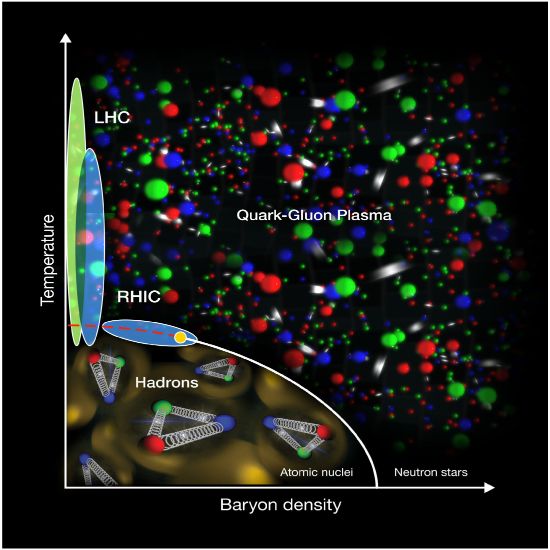

QCD phase diagram: current and future experiments

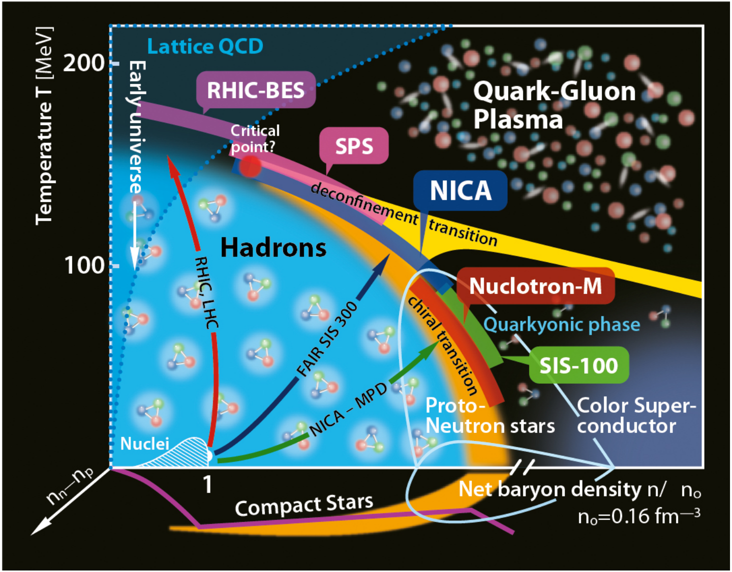

QCD phase diagram

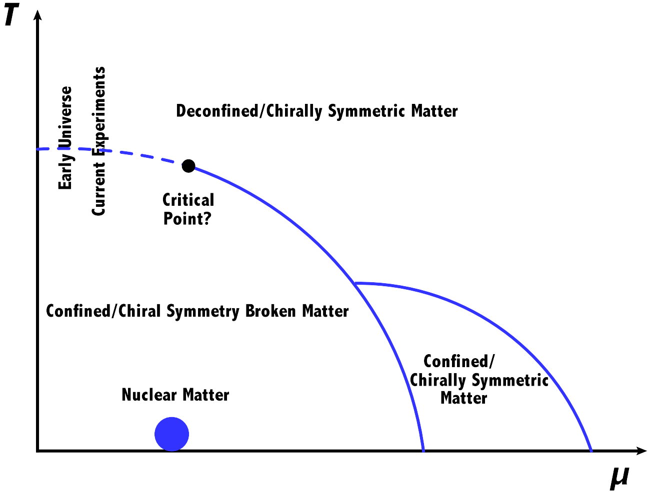

QCD phase diagram, main features:

- It is an analytic crossover for $\mu = 0$ (there are no divergences in thermodynamic quantities). There are no symmetries to break. It would be a real phase transition for massless quarks.

- For $T = 0$ it is a first order phase transition

- The first order phase transition turns into a crossover somewhere in the middle

Light quark condensate $\langle\bar{\psi}\psi\rangle$ from lattice QCD

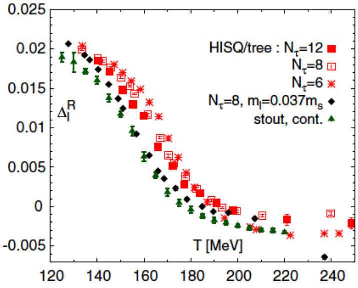

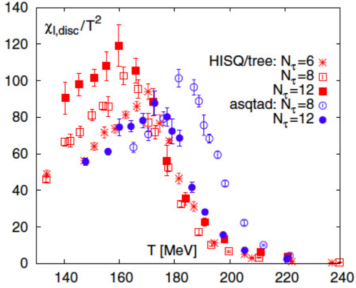

A. Bazavov *et al.*, Phys. Rev. D **85**, 054503 (2012).

Critical temperatures from lattice QCD for $\mu = 0$

T_c from susceptibility's peak for 2+1 flavors using different kinds of fermion representations. Values show some discrepancies:

- MILC collaboration: $T_c = 169(12)(4)$ MeV.
- BNL-RBC-Bielefeld collaboration: $T_c = 192(7)(4)$ MeV.
- Wuppertal-Budapest collaboration has consistently obtained smaller values, the last being $T_c = 147(2)(3)$ MeV.
- HotQCD collaboration: $T_c = 154(9)$ MeV.

Differences may be attributed to different lattice spacings

For $\mu_B \neq 0$ matters get complicated: Sign problem

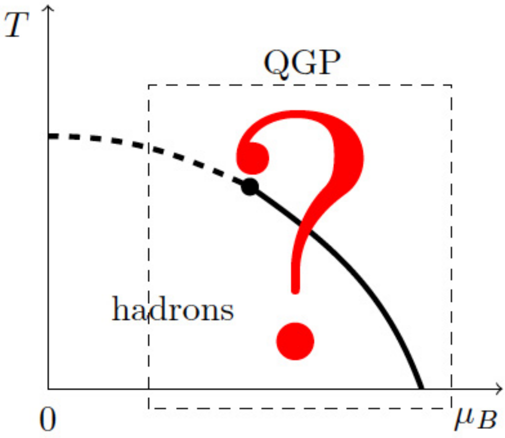

The sign problem

- Lattice QCD is affected by the **sign problem**
- The calculation of the partition function produces a fermion determinant.

$$\text{Det}M = \text{Det}(\not{D} + m + \mu\gamma_0)$$

- Consider a complex value for μ. Take the determinant on both sides of the identity

$$\gamma_5(\not{D} + m + \mu\gamma_0)\gamma_5 = (\not{D} + m - \mu^*\gamma_0)^\dagger,$$

we obtain

$$\text{Det}(\not{D} + m + \mu\gamma_0) = \left[\text{Det}(\not{D} + m - \mu^*\gamma_0)\right]^*,$$

This shows that **the determinant is not real unless $\mu = 0$ or purely imaginary**

The sign problem

For real μ **it is not possible to carry out the direct sampling on a finite density ensemble by Monte Carlo methods**

- It'd seem that the problem is not so bad since we could naively write

$$\mathrm{Det}M = |\mathrm{Det}M| e^{i\theta}$$

- To compute the thermal average of an observable O we write

$$\langle O \rangle = \frac{\int DU e^{-S_{YM}} \mathrm{Det}M \; O}{\int DU e^{-S_{YM}} \mathrm{Det}M} = \frac{\int DU e^{-S_{YM}} |\mathrm{Det}M| e^{i\theta} \; O}{\int DU e^{-S_{YM}} |\mathrm{Det}M| e^{i\theta}},$$

- S_{YM} is the Yang-Mills action.

The sign problem

- Written in this way, the simulations can be made in terms of the *phase quenched theory* where the measure involves $|\text{Det}M|$ and the thermal average can be written as

$$\langle O \rangle = \frac{\langle O e^{i\theta} \rangle_{\text{pq}}}{\langle e^{i\theta} \rangle_{\text{pq}}}.$$

- The average phase factor (also called the average sign) in the **phase quenched theory** can be written as

$$\langle e^{i\theta} \rangle_{\text{pq}} = e^{-V(f-f_{pq})/T},$$

where f y f_{pq} are the free energy densities of the full and the phase quenched theories, respectively and V is the 3-dimensional volume.

- If $f - f_{pq} \neq 0$, the average phase factor decreaces exponentially when V grows (thermodynamical limit) and/or when T goes to zero.

Under these circumstances the signal/noise ratio worsens.
This is known as the severe sign problem

The curvature κ of the transition line

$$\frac{T_c(\mu_B)}{T_c(\mu_B=0)} = 1 - \kappa \left(\frac{\mu_B}{T_c(\mu_B)}\right)^2 + \lambda \left(\frac{\mu_B}{T_c(\mu_B)}\right)^4$$

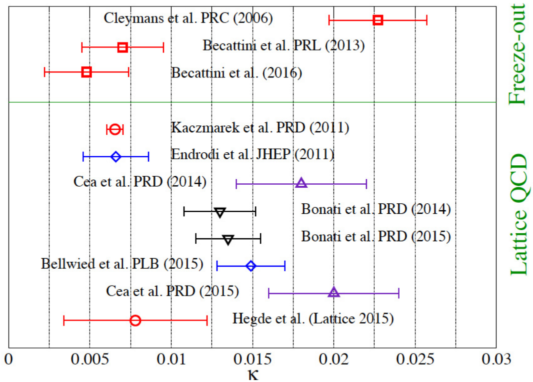

Chiral transition and freeze out curve

Chiral transition, hadronization and freeze-out

LGT: $T_c(\mu_B) = 154(9)(1 - [0.006; 0.014](\mu_B/T)^2)\mathrm{MeV}$

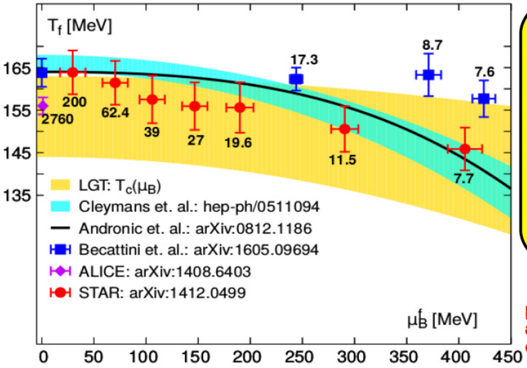

phenomenological freeze-out / hadron-ization curve, QCD transition line and experimental data (obtained by <u>assuming the validity of the HRG model</u>) are consistent for

$$\mu_B/T \lesssim 3$$

<u>HOWEVER</u>

physics is quite different at lower and upper end of the current error bar on Tc

→ **probed with net-charge correlations&fluctuations**

F. Karsch, SQM, June 2016 6

QCD phase diagram from analytic continuation

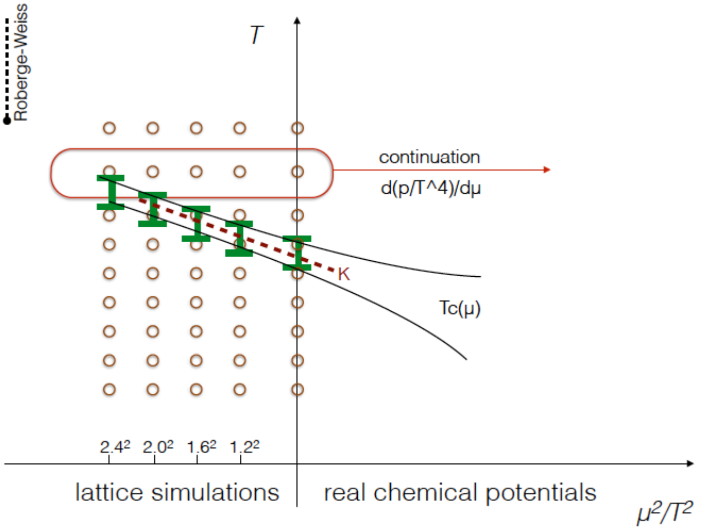

QCD phase diagram from analytic continuation

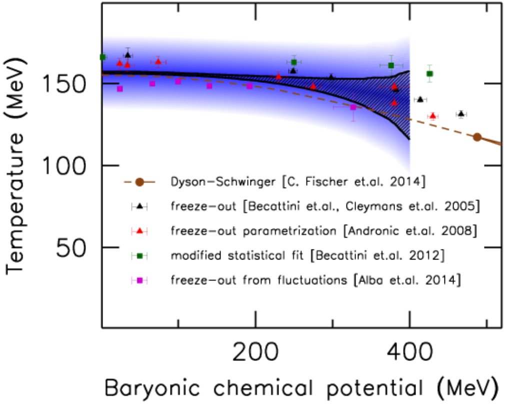

R. Bellwiede, S. Borsanyi, Z. Fodor, J. Gnther, S. D. Katz, C. Ratti, K. K. Szabo, Phys. Lett. B **751**, 559-564 (2015).

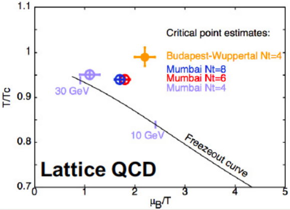

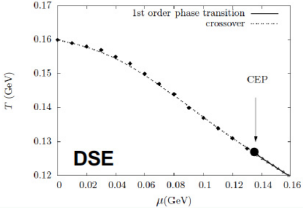

Lattice QCD:

1): Fodor&Katz, JHEP 0404,050 (2004):
$(\mu^E_B, T_E) = (360, 162)$ MeV (Reweighting)

2): Gavai&Gupta, NPA 904, 883c (2013)
$(\mu^E_B, T_E) = (279, 155)$ MeV (Taylor Expansion)

3): F. Karsch ($\mu^E_B / T_E > 2$, CPOD2016)

DSE:

1): Y. X. Liu, et al., PRD90, 076006 (2014).
$(\mu^E_B, T^E) = (372, 129)$ MeV

2): Hong-shi Zong et al., JHEP 07, 014 (2014).
$(\mu^E_B, T_E) = (405, 127)$ MeV

3): C. S. Fischer et al., PRD90, 034022 (2014).
$(\mu^E_B, T^E) = (504, 115)$ MeV

$\mu^E_B = 266 \sim 504$ MeV, $T_E = 115 \sim 162$, $\mu^E_B / T_E = 1.8 \sim 4.38$

Xiaofeng Luo ISMD 2016, Jeju, Korea, Aug. 29-Sept. 2, 2016 3 / 18

CEP location $\mu_B/T > 2$ for 135 MeV $< T <$ 155 MeV

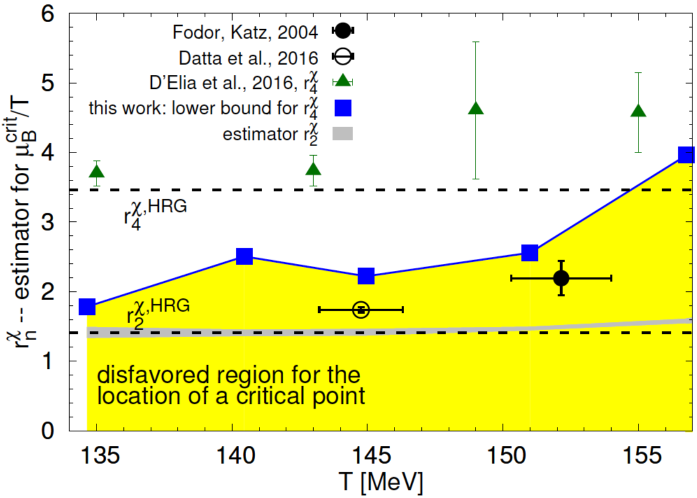

A. Bazavov, *et al.*, Phys. Rev. D **95**, 054504 (2017).

Linear Sigma Model with Quarks

$$\mathcal{L} = \frac{1}{2}(\partial_\mu \sigma)^2 + \frac{1}{2}(\partial_\mu \vec{\pi})^2 + \frac{a^2}{2}(\sigma^2 + \vec{\pi}^2) - \frac{\lambda}{4}(\sigma^2 + \vec{\pi}^2)^2 + i\bar{\psi}\gamma^\mu \partial_\mu \psi - g\bar{\psi}(\sigma + i\gamma_5 \vec{\tau} \cdot \vec{\pi})\psi,$$

$$\sigma \to \sigma + v,$$

$$\begin{aligned} m_\sigma^2 &= 3\lambda v^2 - a^2, \\ m_\pi^2 &= \lambda v^2 - a^2, \\ m_f &= gv. \end{aligned}$$

Three level potential (vacuum stability)

$$V^{\text{tree}}(v) = -\frac{a^2}{2}v^2 + \frac{\lambda}{4}v^4$$

$$v_0 = \sqrt{\frac{a^2}{\lambda}},$$

$$V^{\text{tree}} = -\frac{a^2}{2}v^2 + \frac{\lambda}{4}v^4 \to -\frac{(a^2 + \delta a^2)}{2}v^2 + \frac{(\lambda + \delta\lambda)}{4}v^4.$$

δa^2 and $\delta\lambda$ constants to be determined from the properties of the phase transitions at $(\mu_B = 0, T^c(\mu_B = 0))$ and $(\mu_B^c(T = 0), T = 0)$.

M. E. Carrington, Phys. Rev. D **45**, 2933

One-loop boson and fermion effective potential

$$V^{(1)\mathrm{b}}(v,T) = T\sum_n \int \frac{d^3k}{(2\pi)^3} \ln D(\omega_n,\vec{k})^{1/2},$$

$$D(\omega_n,\vec{k}) = \frac{1}{\omega_n^2 + k^2 + m_b^2},$$

$$V^{(1)\mathrm{f}}(v,T,\mu_q) = -T\sum_n \int \frac{d^3k}{(2\pi)^3} \mathrm{Tr}[\ln S(\tilde{\omega}_n - i\mu_q,\vec{k})^{-1}],$$

$$S(\tilde{\omega}_n,\vec{k}) = \frac{1}{\gamma_0\tilde{\omega}_n + \not{k} + m_f}.$$

$\omega_n = 2n\pi T$ and $\tilde{\omega}_n = (2n+1)\pi T$ are
the boson and fermion Matsubara frequencies

Ring-diagrams effective potential

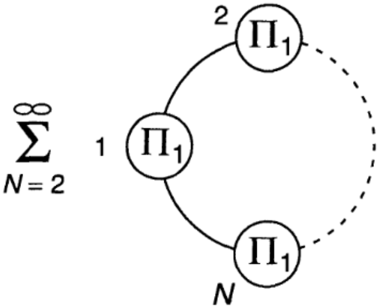

$$V^{\text{Ring}}(v, T, \mu_q) = \frac{T}{2}\sum_n \int \frac{d^3k}{(2\pi)^3} \times \ln[1 + \Pi(m_b, T, \mu_q) D(\omega_n, \vec{k})]$$

$\Pi(m_b, T, \mu_q)$ is the boson's self-energy.

Diagrams contributing to bosons' self-energies

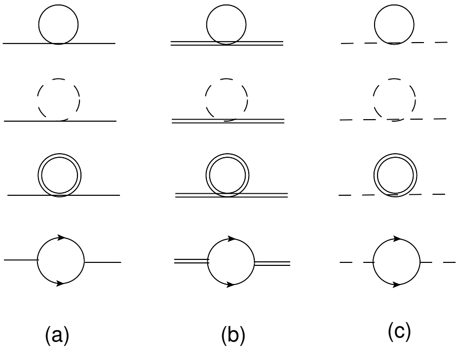

$$\Pi(T,\mu_q) = \quad -N_f N_c g^2 \frac{T^2}{\pi^2}[\mathrm{Li}_2(-e^{\mu_q/T}) + \mathrm{Li}_2(-e^{-\mu_q/T})] + \frac{\lambda T^2}{2}.$$

Effective potential: High T approximation

$$
\begin{aligned}
V^{\text{eff}}_{\text{HT}} &= -\frac{(a^2+\delta a^2)}{2}v^2 + \frac{(\lambda+\delta\lambda)}{4}v^4 \\
&+ \sum_{b=\sigma,\bar{\pi}} \Big\{ -\frac{m_b^4}{64\pi^2}\Big[\ln\Big(\frac{a^2}{4\pi T^2}\Big) - \gamma_E + \frac{1}{2}\Big] \\
&- \frac{\pi^2 T^4}{90} + \frac{m_b^2 T^2}{24} - \frac{(m_b^2+\Pi(T,\mu_q))^{3/2} T}{12\pi} \Big\} \\
&+ \sum_{f=u,d} \Big\{ \frac{m_f^4}{16\pi^2}\Big[\ln\Big(\frac{a^2}{4\pi T^2}\Big) - \gamma_E + \frac{1}{2} \\
&- \psi^0\Big(\frac{1}{2}+\frac{\mathrm{i}\mu_q}{2\pi T}\Big) - \psi^0\Big(\frac{1}{2}-\frac{\mathrm{i}\mu_q}{2\pi T}\Big)\Big] \\
&- 8 m_f^2 T^2 \Big[\mathrm{Li}_2(-e^{\mu_q/T}) + \mathrm{Li}_2(-e^{-\mu_q/T})\Big] \\
&+ 32 T^4 \Big[\mathrm{Li}_4(-e^{\mu_q/T}) + \mathrm{Li}_4(-e^{-\mu_q/T})\Big] \Big\}
\end{aligned}
$$

Effective potential: Low T approximation

$$
\begin{aligned}
V_{\rm LT}^{\rm eff} &= -\frac{(a^2+\delta a^2)}{2}v^2 + \frac{(\lambda+\delta\lambda)}{4}v^4 \\
&- \sum_{i=\sigma,\bar{\pi}} \left\{ \frac{m_i^4}{64\pi^2}\left[\ln\left(\frac{4\pi^2 a^2}{(\mu_b+\sqrt{\mu_b^2-m_i^2})^2}\right)-\gamma_E+\frac{1}{2}\right] - \frac{T^2\mu_b}{12}\sqrt{2\mu_b^2-5m_i^2} \right.\\
&\left. - \frac{\mu_b\sqrt{\mu_b^2-m_i^2}}{24\pi^2}(2\mu_b^2-5m_i^2) - \frac{\pi^2 T^4\mu_b}{180}\frac{(2\mu_b^2-3m_i^2)}{(\mu_b^2-m_i^2)^{3/2}} \right\} \\
&+ N_c \sum_{f=u,d} \left\{ \frac{m_f^4}{16\pi^2}\left[\ln\left(\frac{4\pi^2 a^2}{(\mu_q+\sqrt{\mu_q^2-m_f^2})^2}\right)-\gamma_E+\frac{1}{2}\right] - \frac{T^2\mu_q}{6}\sqrt{\mu_q^2-m_f^2} \right.\\
&\left. - \frac{\mu_q\sqrt{\mu_q^2-m_f^2}}{24\pi^2}(2\mu_q^2-5m_f^2) - \frac{7\pi^2 T^4\mu_q}{360}\frac{(2\mu_q^2-3m_f^2)}{(\mu_q^2-m_f^2)^{3/2}} \right\}
\end{aligned}
$$

Effective potential (High and Low T)

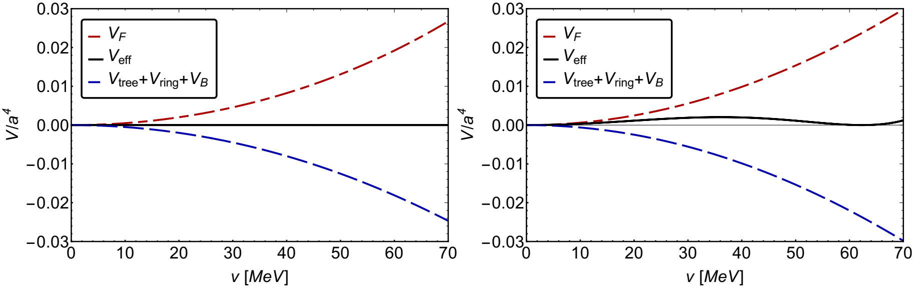

A. A., S. Hernández-Ortiz, L. A. Hernández, arXiv:1710.09007.

$\mu_q = \mu_b$

Upper line: $T_0^c(\mu_q = 0) = 175$ MeV and $\mu_q^c(T = 0) = 350$ MeV
Lower line: $T_0^c(\mu_q = 0) = 165$ MeV and $\mu_q^c(T = 0) = 330$ MeV
$0.80 < \lambda < 0.91$ and $1.56 < g < 1.62$

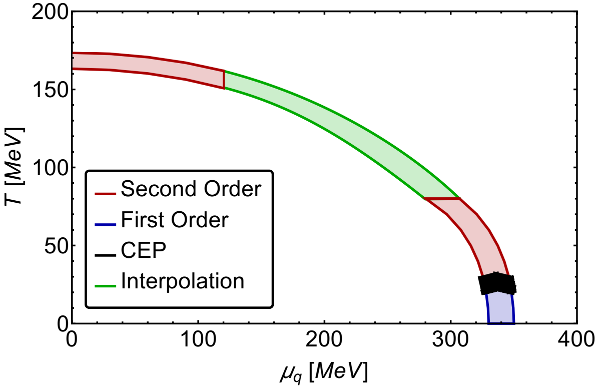

A. A., S. Hernández-Ortiz, L. A. Hernández, arXiv:1710.09007.

$\mu_q = 2\mu_b$

Upper line: $T_0^c(\mu_q = 0) = 175$ MeV and $\mu_q^c(T = 0) = 350$ MeV
Lower line: $T_0^c(\mu_q = 0) = 165$ MeV and $\mu_q^c(T = 0) = 330$ MeV
$0.85 < \lambda < 1.40$ and $1.53 < g < 1.69$

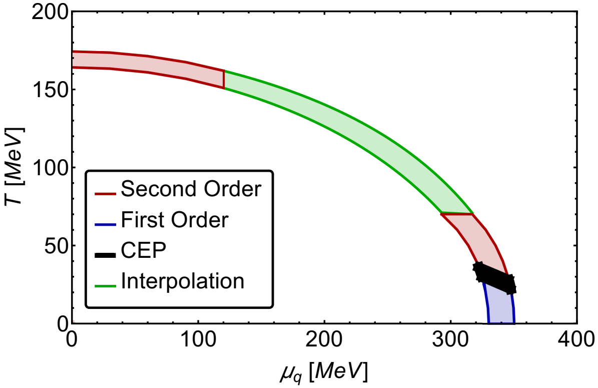

A. A., S. Hernández-Ortiz, L. A. Hernández, arXiv:1710.09007.

$\mu_q = 0.5\mu_b$

Upper line: $T_0^c(\mu_q = 0) = 175$ MeV and $\mu_q^c(T = 0) = 350$ MeV
Lower line: $T_0^c(\mu_q = 0) = 165$ MeV and $\mu_q^c(T = 0) = 330$ MeV
$0.79 < \lambda < 1.10$ and $1.57 < g < 1.62$

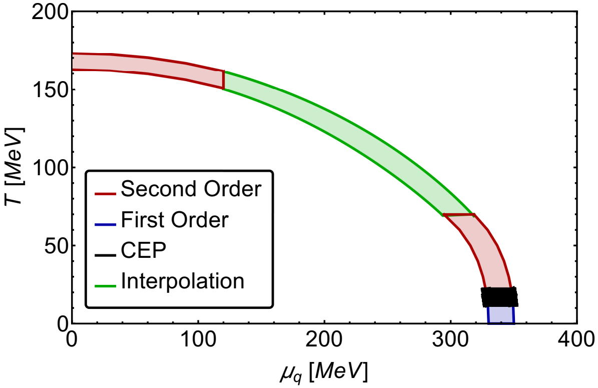

A. A., S. Hernández-Ortiz, L. A. Hernández, arXiv:1710.09007.

Conclusions

- Main goal of future experiments in the field heavy-ion physics is to study QDC at finite baryon density.
- Many challenges. Of particular importance to determine whether there is a CEP.
- Lattice QCD still far from providing an answer. Need theoretical hindsight.
- Effective models are useful tools to gain insight into the properties of strongly interacting matter.
- Linear sigma model is one possibility: Complete exploration allowing the couplings to bear baryon density and temperature effects. Stay tunned.

Happy Birthday Guy! Congratulations for the many years of successes! May it be many more!